OPTIMIZATION OF MECHANICAL PROPERTIES OF POROUS MATERIALS

S. Firstov, Yu. Podrezov

ABSTRACT

Possible ways to improve mechanical property of porous materials, depending on volume fraction of pores, are discussed. The first possibility is an enhancement of fracture toughness of porous material by increasing the volume fraction of pores. The second is the growth of relative stiffness of high-porous systems. The third case is to increase the absorbing capacity of strain energy at a high porosity. The sensitivity of these effects to the morphology of porous space, and structure of solid phase, is analysed. The methods of structure optimisation in order to obtain maximum effects are proposed. Solid state structure and porous space morphology were taken into account. There is a good agreement between theoretical calculation and experimental data. Requirements of designers will always be met if the morphology of porous structure and mechanical property of basis metal is optimal.

Keywords: porous materials, fracture toughness, relative stiffness, structural effect, work hardening, damper stress

INTRODUCTION

Pores are one of the structural elements of a material. Porosity can be a result of material technology as well as being regulated consciously, for example, when producing filtered or low-weight materials. In the first case, one usually tends to get rid of porosity by improving material technology or realising special treatments, for example, isostatic hot-pressing. In the second case, special technologies are worked out for obtaining regulated porosity. With this aim, both a simple combination of powder pressing condition or sintering modes and a special heat treatment are used in powder metallurgy. Therefore, both investigations of porous material structure and the influence on physical-mechanical properties of the materials are of considerable interest.

A number of physical properties (for example, thermal expansion coefficient) do not depend on porosity, other properties (for example, density) depend on porosity linearly. The mechanical properties of sintered materials are drastically reduced when the porosity increases. In particular, the following formulas have been derived in a number of publications [1-6]

$$\sigma(\theta)_y = \sigma_{y0}(1-\theta)^m, \tag{1}$$

$$\sigma(\theta)_f = \sigma_{f0} e^{-b\theta}, \tag{2}$$

$$\sigma(\theta)_y = \frac{\sigma_{y0}(1-\theta)^2}{\sqrt{4}} - 3\theta, \tag{3}$$

Sergey Firstov, Yuriy Podrezov, Institute for Problems in Materials Science of the Academy of Sciences of Ukraine, Department of Physics Strength and Plasticity, Kiev, Ukraine

$$\sigma(\theta)_f = K_y d^{-\frac{1}{2}} e^{-b\theta}, \quad (4)$$

$$E(\theta) = E_0 (1-\theta)^m, \quad (5)$$

where θ is porosity; σ_{y0} and $\sigma(\theta)_y$ are the yield stresses of compact and porous material; σ_{f0} and $\sigma(\theta)_f$ - the same for fracture stresses; d is the grain size; K_y – Hall-Petch coefficient; E_0 and E(θ) are the elastic modulus of compact and porous material; b and m – constant.

These dependencies agree with the experiment as to the porosity values of θ ≤ 30%. Some more complicated dependencies of the properties have been proposed for the range θ ≤ 60% [3-8], and for high porous materials, the percolation theory equations is employed [9].

Balshin supposed [1,2] that the dimensionless coefficient

$$\alpha = \frac{E(\theta)}{E_0}$$

characterises the relative fraction of load carrying (critical) material. Balshin suggested that

$$\alpha = \frac{E(\theta)}{E_0} \approx \frac{S(\theta)}{S_0},$$

where $S(\theta)$ and S_0 are the properties of porous and compact bodies which are proportional to the "critical" fraction (for example, tensile strength).

Krasovsky [10] considered, however, that the relation

$$\frac{E(\theta)}{E_0}$$

characterises a mean value of the "critical" fraction, but that

$$\frac{\sigma_f(\theta)}{\sigma_{f0}}$$

is determined by the weakest fraction, therefore,

$$\frac{E(\theta)}{E_0} \geq \frac{\sigma_f(\theta)}{\sigma_{f0}}.$$

Further improvement of the micromechanical model of fracture of powder materials was made by M. Šlesár [11]. He defined new important structural parameters of fracture PM materials: plain porosity θ_x and neck porosity θ_n.

There is a somewhat unusual influence of the dimension and shape of the specimens (scale factor) on the properties of sintered porous bodies. As it has been shown in [12], the strength is reduced if the specimen length increases. But it is slightly enhanced with increasing cross-section area.

It should be noted that the theoretical investigation of the porosity effect on properties (with some restrictions imposed in the models used for calculations) can be carried out quite correctly. However, experimental investigations face a number of additional difficulties. Specifically, using a different variant of treatment technique for porous materials, experimenters involuntarily change other structural parameters: grain size, state of interfaces, impurity distribution. The structural aspects of the physical mechanisms of deformation and fracture of powder materials have been analysed in our book with M. Šlesár, Ľ. Parilák et al. [11]. In this book, the problems of structural

sensitivity of the yield point of powder materials; strain hardening of powder solids; the porosity effect on fracture mechanisms and on other properties; mechanical properties in the case of interparticle mechanisms of fracture were also studied. Those points were developed in our last works [14-17].

Practical application of high-porous materials as an element of construction is more really in the cases when the mechanical behaviour of porous materials improves with a rise of porosity. We have tried to find the ways to improve mechanical properties of porous materials. Some possible cases will be discussed in this article. The sensitivity strengthening effect on the structure of porous space and solid phase will be analysed, and structural optimisation of high porous material will be proposed in the context of our previous results.

FRACTURE TOUGHNESS OF POWDER MATERIALS UNDER BRITTLE - DUCTILE TRANSITION TEMPERATURE

The first example is fracture toughness increasing in porous materials at a brittle-ductile transition (BDT) temperature. This effect was demonstrated on the sintering powder iron testing at 77 K in [13]. Figure 1 displays the fracture toughness alteration with porosity in powder iron materials, with various porosity and impurities. In all cases, the maximum value of fracture toughness is revealed at critical porosity θ_{cr}, which is characterised by a transition of fracture mechanism from cleavage under low porosity, to ductile under higher porosity.

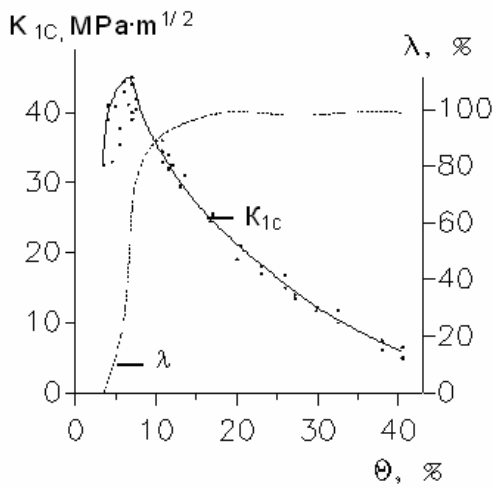

Fig.1. Dependence of fracture toughness K_{1C} and portion of tough fracture mode λ on porosity θ for sintered iron powder

According to this data, the brittle-ductile model for BCC-powder materials with various porosity and impurities was proposed in [18]. Transition from brittle to ductile fracture occurs at the critical porosity θ_{cr}, which is determined from the condition of equality of fracture toughness for both brittle and ductile mechanisms.

For cleavage fracture mechanism, the dependence of fracture toughness on porosity may be given in the form

$$K_{1c}^{cl}(\theta) = \sigma_f(\theta)\sqrt{\pi d}\ , \tag{6a}$$

where d is grain size and $\sigma_f(\theta)$ is

$$\sigma_f(\theta) = \sigma_{cl0}(1-\theta)\cdot\left(1+\frac{\sigma_f^2(\theta)}{2\pi\sigma_y^2(\theta)}\right), \tag{6b}$$

σ_{cl0} is microcleavage stress of compact materials which is determined under BDT temperature (T_x) from the relation $\sigma_{cl0} = \sigma_{y0}(T_x)$.

For a ductile fracture the Hahn-Rosenfield relation [19] was used, taking into account the dependence of mechanical properties on porosity

$$K_{1C}^{duc}(\theta) = n\sqrt{\frac{3}{2}\pi d E(\theta)\sigma_y(\theta)\varepsilon_r(\theta)}, \tag{7}$$

where n is the strengthening exponent; E is the elastic modulus; ε_r is the critical deformation.

K_{1c} - θ - T topogram was calculated from this equation. Theoretical curves K_{1c} vs. θ for 77 K, 123 K and 293 K are in a good agreement with experimental data.

Variation of fracture toughness with porosity depends on the material structure and test temperature. In terms of our model presented in [18], the form of curves K_{1c} vs. θ can be predicted from the relation for σ_{cl0} and σ_{y0} of initial nonporous material. Experimental data show that, under BDT condition $\sigma_{cl0} = \sigma_y$, different BCC materials demonstrate a nonmonotonous K_{1c} vs. θ dependence similar to the curves in Fig.2.

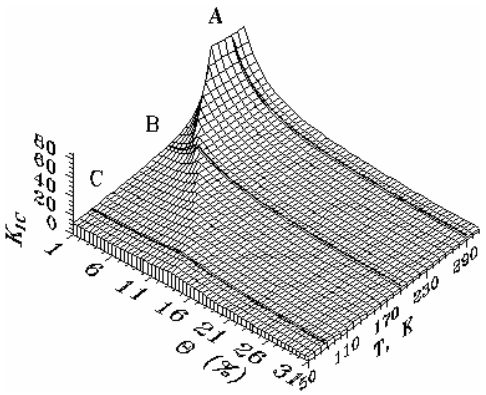

Fig.2. Fracture toughness as a function of porosity θ and temperature T for iron-based powder material (Fe - 0.6% C), characterised by microcleavage stress σ_{cl} = 650 MPa.

Thus, investigation of mechanical behaviour of various materials under an isomechanical condition, allow general regularities of material structure effect on fracture processes and K_{1c} formation to be established. This effect was employed to increase fracture toughness of cold resistance steels and to improve fracture resistance of chromium, molybdenum and tungsten powder alloys [20], which reveal BDT near room temperature. Ľ. Parilák et al. [13] found the same strengthening effect of porosity on BDT under an impact toughness test in iron.

INCREASING OF FRACTURE TOUGHNESS OF BRITTEL MATERIALS CONNECTING WITH BLUTTING OF CRACK

S. Firstov and A. Vasilev [21] showed that, in contrast to the generally accepted facts of negative influence of pores on the fracture toughness, the toughening effect for brittle powder materials can exist. In investigations on glass [22], a maximum of K_{1c} vs. porosity curve has been obtained. The maximum has corresponded to the similar porosity interval. A formula for the dependence K_{1c} vs. porosity in this case

$$K_{1c}(\theta) = K_{1c0}(1-\theta^m)\sqrt{1+(\rho_\pi/\rho_0-1)^w}\,, \tag{8}$$

where K_{1c0} - fracture toughness of the compact material, ρ_π – blunted crack tip radius, ρ_0 - atomic sharp crack tip radius, w – probability that crack tip has a blunting of the order d, $w \cong (\theta/\theta_K)^{2m}$ when $0<\theta<\theta_K$, $w = 1$ when $\theta>\theta_K$ and θ_K – critical porosity value. The calculated dependencies of K_{1c}/K_{1c0} vs. porosity at different values of ρ_π/ρ_0 ratio are shown in Fig.3.

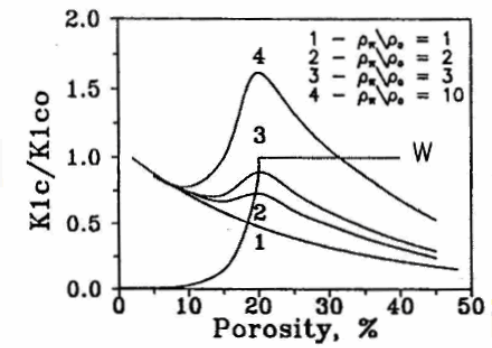

Fig.3. The predicted dependence of fracture toughness of porous body, with different ratios between pores radii and sharpness of notch tips, on porosity for cleavage and intergranular fracture mechanisms. W is the probability of the entry of the notch tip into pores space.

Figure 3 shows the predicted dependence of fracture toughness on porosity for different values of the radius of fracture initiating notch ρ_π. It is seen that the probability of the full blunting of the notch tip by pores takes place at a porosity content higher than 20%. In increases from 0 to 1, porosity increase from 10 to 20%, is in a full accordance with the experimental results [22]. It is also seen that by increasing the notch radius, even up to 10 times, i.e. to 5-7 micrometers, the fracture toughness of a brittle material increases nearly twice.

Such fracture mechanisms result in a nonlinear loading diagram. In [23] we tried to solve a physical problem of the description of non-elastic behaviour of ceramic as a stochastic process of the cracking of separate structural elements. The dependence of the normalised stress on the normalised strain is shown in Fig.4.

There are four stages of process. The first stage is loading without microcracking. The second stage is a stable, non-localised microcracking before the stress maximum. The third stage is a stable localised microcracking after the stress maximum. The fourth stage is an unstable (catastrophic) fracture. In fact, the third and fourth stages are during a very short time as a result of fracture localisation. Hence, these stages are invisible in practice. The stages of stable non-localised microcracking and stable localised microcracking, are before the strain energy density maximum. The stage of unstable (catastrophic) fracture is after the maximum in Fig.4. There are some features of the microcracking process under

bending the compacts, or a low porous ceramic. The third state is absent in this case. The second stage of scattered microcracking is up to the stage of catastrophic fracture.

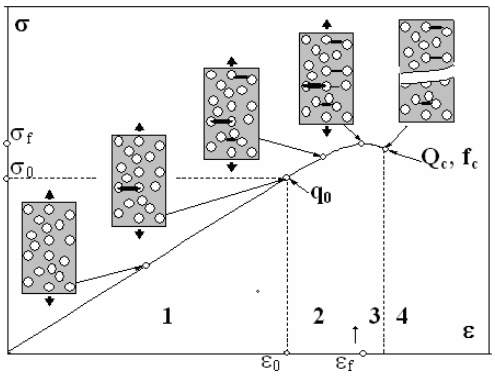

Fig.4. Schematic illustration of the dependence of the normalised stress on the normalised strain for porous material: 1 - loading without microcracking; 2 - stable nonlocalised microcracking stage; 3 - stable localised microcracking stage; 4 - unstable (catastrophic) fracture stage.

In contrast, in the case of high porous ceramic, all above-mentioned states are observed clearly. The true load-deflection diagram of porous (39%) alumina was investigated in [24] and is presented in Fig.5. This diagram is in good agreement with the schematic illustration (Fig.4). The deformational process of comparatively brittle ceramics is the process of crack accumulation in its structure caused by an increase in the length of cracks as well as their number. This process requires an additional energy and it is additional dissipation of elastic strain energy.

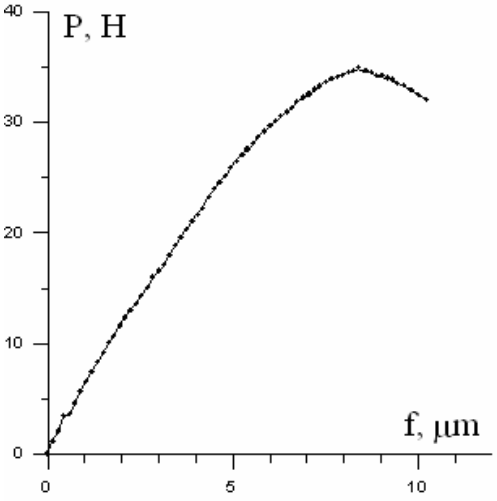

Fig.5. “Load – deflection” curve for porous alumina (θ = 38%)

Within the framework of the model described in [23], the modelling of the mechanical behaviour of porous ceramics may be conducted. Both the structural parameters

(grain size) and statistic distribution of pores are used as initial data for further calculation. This modelling process makes it easier to determine the dependence of the number of cracks per unit area on the level of stresses applied. The volume of the fractured structure elements, or the density of microcracks, can be expressed by the product of the number of cracks or fractured structure elements in the volume unit, and mathematical expectation of the volume of the fracture structure element.

Practical application of the results of increasing fracture toughness of porous materials has some restrictions because of the relatively low weight effect. Other examples have not such limitations. High porous materials have an essential advantage in wide porosity interval when the construction weight is the main parameter, and its sizes can vary.

RELATIVE STIFFNESS OF HIGHPOROUS MATERIALS

In [16,17,25] the effect of the porous space structure on the relative stiffness of high-porous powder materials was analysed. The most simple and cheap way of obtaining high-porous materials by means of powder metallurgy methods, is pressing and sintering of basic powder with pore-forming powder. The distinguishing feature of the pore space structure of the given class of materials, is that the system of large pores is matrical, and that of the small pores located between the powder particles is statistical. Ideal matrisity is achieved when the size of the pore-forming particles is many times larger than that of the powder particles.

Quantitative evaluation of the effect of structural factors on several relative mechanical parameters was made on the basis of experimental data and phenomenological analysis. The influence of structural parameters on relative properties of highporous powder and compact materials was obtained in analytical form.

Parameter k_{km} is the relative stiffness for the same weight

$$k_{km} = \frac{k_\theta}{k_0} = \frac{E(\theta)}{E_0} \cdot \left(\frac{1}{1-\theta} \right)^3 , \tag{9}$$

where k_0 is stiffness of compact material and k_θ is stiffness of porous material. Parameter k_{ym} is the gain in yield load for the same weight

$$k_{ym} = \frac{P_y}{P_0} = \frac{\sigma_0(\theta)}{\sigma_{y0}(1-\theta)^2} = \frac{E(\theta)}{E_0(1-\theta)^2} , \tag{10}$$

where P_y is yield load of porous materials; P_0 - yield load of solid phase. According to percolation theory [17], parameter E_θ/E_0 may be given in the form

$$E(\theta) = E_0 \left(1 - \frac{\theta}{\theta_c} \right)^\beta , \tag{11}$$

where θ_c is the porosity of the percolation threshold when effective modulus becomes zero; β is the critical exponent that can be theoretically predicted for various physical properties [9].

The influence of the ratio of the pore forming material and powder particle sizes, m, and the volume fraction of pores, θ, on relative stiffness in pore-forming powder materials is shown in Fig.6.

The relative stiffness maximum ($k_{km} = 6$) is observed in the optimal structural state (for biporous nickel whose structural parameters are $\theta = 70\%$ and $m = 50$). It means that, under equal loads, such a porous beam has one-sixth as large deflection as a compact beam that has the same weight. Or under condition of equal deflection, the porous beam has load six times as much as that of the compact beam, the effect for other biporous materials is

lesser. It is important that the powder materials without pore forming do not show the increase of relative stiffness.

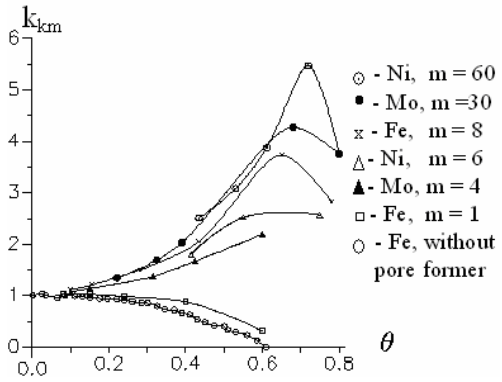

Fig.6. Dependence of relative stiffness k_{km} on porosity θ

MAXIMUM ENERGY ABSORPTION CRITERION

Another example is connected with the unique ability of high porous materials to absorb deformation energy under a small damping stress. Such materials have priority in protective constructions. The absorption energy depends strongly on the apparent porosity. If the porosity is too high, the form crushes before impact energy is sufficiently absorbed. If the porosity is too low, the stress in the form exceeds given critical value at low absorbed energy. The example of compressive stress-strain curves (θ-ε) of foamed aluminium for different densities is shown in Fig.7. Vertical lines on the scheme (Fig.8) correspond to bounds between the stages of easy and strong deformation strengthening. Structural optimisation of high porous material allows reaching the maximum value of work hardening. From this point of view, it is necessary to know the rule of the strengthening of based metals, the influence of porosity on the stress-strain curve and on the deformation degree at the end of the easy deformation stage (Fig.8).

According to [27], damper efficiency is determined by the ratio of real energy of plastic deformation and the maximal one under a given degree of deformation and stress.

$$\phi = \frac{\int_0^l F dl}{F_{max} L}, \qquad (12)$$

where F is the alternating load, l is the alternating displacement, F_{max} is the maximal load and L is the maximal displacement according to compressive curve. The high porous materials have maximal efficiency at the easy deformation stage. According to experimental data and theoretical investigation [28], stress vs. strain dependence in this stage may be expressed as a linear function. Taking into account this fact and Eq.12, the deformation degree at the end of the easy deformation stage can be determined as point on the stress-strain curve for which inequality $d^2\sigma/d\varepsilon^2>0$ is satisfied.

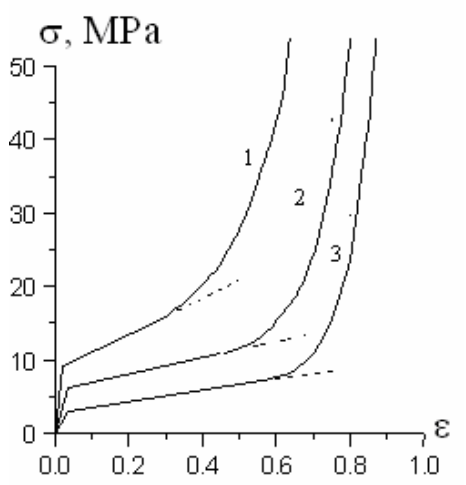

Fig.7. Stress-strain dependence of foam aluminium at different porosity θ under compression: 1 - θ = 0.74; 2 - θ = 0.84; 3 - θ = 0.89

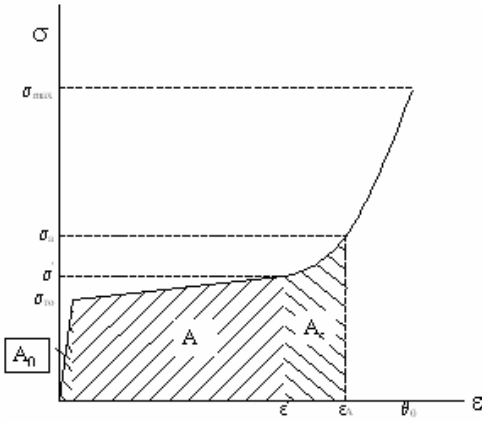

Fig.8. Stress-strain dependence of high-porous material under compression

Ashby and Gibson [28] proposed a cubic form of unit cell for high porous materials. An elastic bending of the walls takes place at the first stage of deformation. At the second stage, plastic bending of the walls occurs up to the moment when opposite walls touch one to another. The walls crush, and collapse comes about in the third stage. According to this deformation model, there is no lateral spreading on the second stage, so the value of porosity in deformed material and the true compressive deformation degree is connected by simple relation:

$$\varepsilon = \frac{\theta_0 - \theta}{1 - \theta}, \tag{13}$$

where ε is the true compressive deformation degree, θ_0 and θ are the initial and current value of porosity under compression respectively.

The influence of the initial porosity on the deformation degree, which corresponds to the end of the easy deformation stage of the deformation curve, can be obtained from analysis of evolution of the unit cell under deformation. Since the three-dimensional variant of the unit cells deformation is very difficult for geometrical construction in [29], we use a more simple two-dimensional cell, which has double the size of lateral walls. Doubling the walls is a possibility to take into account all lateral walls bending in a cubic cell. If H is the height of cell, and h/2 is the thickness of walls, the initial porosity can then be written as follows:

$$\theta_0 = 1 - 3\frac{h}{H}, \tag{14}$$

Unit cell changes its form after deformation. The deformation in the contact moment is

$$\varepsilon' = \frac{H - H'}{H}, \tag{15}$$

where H' - height of cell at this moment. Geometrical construction shows that H' is connected with geometrical parameters H and h of unit cell by relation

$$H' = \sqrt{3h(2H - h)} \,. \tag{16}$$

From Eqs.14, 15 and 16 the influence of initial porosity on the deformation degrees at the end of easy deformation stage can be obtained in the form:

$$\varepsilon' = 1 - \sqrt{\frac{(1-\theta_0)(5+\theta_0)}{3}} \,. \tag{17}$$

The experimental values of ε' parameter for foamed aluminium and high porous powder nickel as function of θ_0 are shown in Fig.9. The Eq.17 is in good agreement with experimental data.

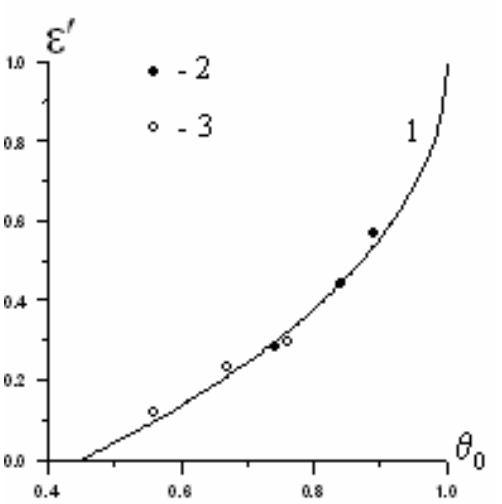

Fig.9. Dependence of strain, corresponding to transition from the second to the third strain stage, on porosity: 1 - calculation according to Eq.3; 2 - experimental data for foam aluminium; 3 - experimental data for high-porous nickel

In [13] we proposed a method to analyse strain hardening curves, allowing for features of deformation behaviour connected with both structure evolution of the solid phase, and porosity alteration, in the deformation process. When investigating strain hardening of porous material in connection with structure transformation in the deformation process, it is necessary to take into account two interrelated processes: the evolution of dislocation structure of the solid phase, and porous structure alteration.

The contribution of solid phase structure is characterised by its deformation stress σ_0^{sph}. This characteristic, like true deformation stress of compact material, can be used for investigation of the physical parameters of strain hardening. The dependence σ_0^{sph} - e has the stage character, the micromechanisms of strain hardening of the materials being invariable within the studied porosity interval. According to [30], porosity contribution to strain hardening of powder material is taken into account by the parameter $E(\theta)/E_0$. This parameter is sensitive to pore structure evolution. The dependence $E(\theta)/E_0 = f(\varepsilon)$ of materials studied under conditions of uniaxial tension and compression, has a nonmonotonous character which is explained by the appearance of a lateral mode of

discompaction under tension, and by the accelerated growth of contact area at the transition of open porosity to the closed one under compression.

The strain hardening curves of foamed materials has linear hardening at the second stage of deformation that can be calculated from the equation

$$\sigma = (\sigma_{y0} + N_0 \varepsilon) E(\theta) / E_0 , \tag{18}$$

where σ_{y0} is the yield point and N_0 is the strain strengthening coefficient of the cell wall material. According to percolation theory [9], parameter $E(\theta)/E_0$ may be given in the form of Eq.11.

Taking into account Eqs.11, 18, the density of deformation energy on easy deformation stage may be calculated from the equation:

$$A = \left(\sigma_{y0} + \frac{N_0}{2} \varepsilon' \right) \left(1 - \frac{\theta_0}{\theta_c} \right)^{\beta} \varepsilon' , \tag{19}$$

where ε' is determined from Eq.17. Parameters θ_c, θ_0 and β characterise sensitivity of absorbed energy to porous space morphology; on the other hand, σ_{y0} and N are determined by microstructure of solid state material. Since Eq.19 is useful for structural optimisation of high porous materials in order to determine maximum absorbed energy value.

As an example we determine the optimal porosity of formed aluminium and high porous powder nickel. The parameters for foamed aluminium are:

$\theta_c \approx 1$, $\beta \approx 1.73$, $E_0 = 7.3$ GPa, $\sigma_{y0} = 100$ MPa, $N_0 = 270$ MPa;

for high porous powder nickel according to [29], the values of parameters are:

$\theta_c = 0.83$, $\beta \approx 1.16$, $E_0 = 20.4$ GPa, $\sigma_{y0} = 210$ MPa, $N_0 = 2080$ MPa.

Substitution of these parameters in Eq.19 gives dependence of deformation energy on the initial porosity (or density) of the foamed aluminium and high porous powder nickel (Fig.10). The maximum value of deformation energy was calculated from Eq.19 for foamed aluminium as $A = 4.08$ MJ/m^3 for $\theta_0 = 0.71$ and for high porous powder nickel as $A = 13.5$ MJ/m^3 for $\theta_0 = 0.68$. The optimal structural state of high porous materials may also be obtained from condition $\frac{\partial A}{\partial \theta_0} = 0$.

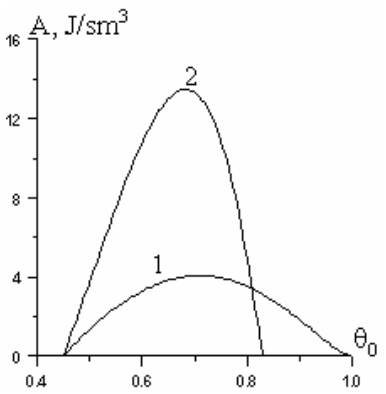

Fig.10. Dependence of plastic strain energy on porosity (or density) under compression: 1 – foam aluminium; 2 – high-porous nickel

If the demanded value of absorbed energy in the protective construction is determined by the designer from special experiments, Eq.19 may be used for a choice of optimal porous morphology (by varying of θ, θ_0 and β) or microstructure of the solid state (by varying σ_{y0} and N_0) of high porous materials. When impact energy absorption is considered, the stress that is attained in the foam is very important.

CRITERION OF MINIMAL STRESS UNDER DAMPER PROCESS

The criterion of a minimal stress σ_{min} under given deformation energy was proposed in [31]. Structural sensitivity of this parameter is shown in Fig.8. The shaded areas correspond to given deformation energy. The stress attained in the foam depends strongly on the initial porosity. It was shown in [31] that minimal stress is attained in high porous materials even in the third stage of deformation (Fig.8).

In this case, structural analysis is necessary to know structural sensitivity of the stress-strain curves of high porous materials in the last linear stage of deformation. Since in the third stage a crush and collapse of the walls takes place, the deformation process is accompanied with lateral spreading and the modulus increasing. In this case, the profile of strain hardening curves has a more complicated character, which is determined by strain hardening curves of the solid phase, porous structure evolution under uniaxial compression, and modulus sensitivity to porosity and its evolution under uniaxial compression. Calculation of nominal deformation stress was executed in [30], with an allowance for sample forming under compression, porosity alteration, and stress redistribution in the bulk of material due to alteration of the pore shape:

$$\sigma_n = \frac{P}{S_0} = \sigma(\varepsilon)\frac{E(\theta,\varepsilon)}{E_0}\frac{1-\Delta\theta}{1-\varepsilon}, \tag{20}$$

where σ_n is the nominal stress, ε and $\Delta\theta$ are relative deformation and porosity alteration corresponding; P is the load under deformation ε, S_0 is the initial area of sample.

The experimental dependencies $E(\theta)/E_0 = f(\varepsilon)$ for porous iron and foam alumina were represented in [30,32]. Elastic stiffness modulus rises steeply when single cell walls start to contact one another. Unfortunately, the stochastic character of crushing process in different points of material creates difficulties for physical interpretation of $E(\theta)/E_0 = f(\varepsilon)$ dependencies. Anisotropic evolution of the porous space under deformation excludes the possibility to obtain correct strain hardening curves by porous changing. Such a correction gives us a higher value of nominal stress then obtained in the experiments. In [15,33] we propose for a correction of strain hardening curves on the third deformation stage to create a new parameter θ_{ef} called effective porosity. This parameter is calculated from equation:

$$\theta_{ef} = \theta_0\left(\frac{\theta_0-\varepsilon}{\theta_0-\varepsilon'}\right)^{1/4}. \tag{21}$$

Taking into account this correction, a nominal stress on the third stage of compressive deformation can be obtained from Eqs.11 and 18 in the form:

$$\sigma(\varepsilon) = \left(1-\frac{\theta_{ef}}{\theta_c}\right)^{\beta}(\sigma_{y0}+N\varepsilon)\cdot \tag{22}$$

For structural optimisation of high porous material according to the minimal stress criteria, it is necessary to solve the equation for deformation energy (Eq.19) and the equations for strain hardening (Eqs.11, 18 and 22) simultaneously. As an example of such a

solution, the dependencies $\sigma_{min} = f(\theta_0)$ for different values of deformation energy are shown in Fig.11a for foamed aluminium, and in Fig.11b for high porous powder nickel. All dependencies have a minimum of stress value under optimal initial porosity. If the absorbed energy increases, the minimal deformation stress increases too, but the optimal initial porosity is less.

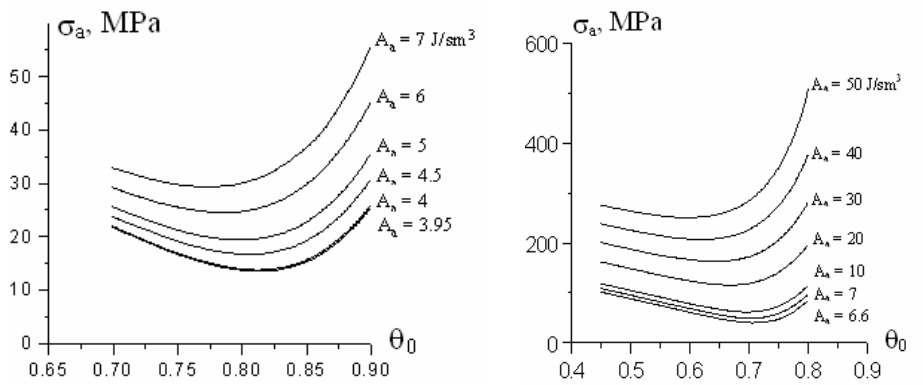

Fig.11. Dependence of maximum damper stress on initial porosity for constant total absorbed strain work under compression: a) foam aluminium; b) biporous nickel

CONCLUSION

In contrast to generally accepted facts of negative influence of pores on strength, there are some cases when mechanical properties increase with a rise of porosity:

- an enhancement of fracture toughness of porous material with an increasing of volume fraction of pores. Depending on fracture mechanisms, this effect can be observed in 10-25% of porosity;
- the growth of relative stiffness of high-porous systems (at 60-80 % porosity);
- the third case is to increase absorbing capacity of strain energy at high porosity.

The proposed model allows choosing the optimal structure of porous material, taking into account properties of solid phase, and morphology of porous space.

References

[1] Balshin, MY.: Scientific fundamentals of powder metallurgy and fibre metallurgy. Moscow : Metallurgy, 1973, in Russian.
[2] Balshin, MY., Kiparisov, SS.: Powder metallurgy fundamentals. Moscow : Metallurgy, 1972, in Russian.
[3] Skorokhod, VV.: Powder materials as the base of refractory metals and compounds. Kiev: Technika, 1977, in Russian.
[4] Andrijevskiy, RA.: Powder Met., 1982, no. 1, p. 37, in Russsian.
[5] Pulvermetallurgie, Sinter – und Verbundwerkstoffe . Ed. W.Shatt. Leipzig : VEB Deutscher Verlag für Grundstoffindustrie, 1977.
[6] Hamiuddin, MD.: Powder Met.Int., vol. 18, 1986, p. 73.
[7] Fedorchenko, IM., Andrijevsky, RA.: Powder metallurgy fundamentals. Kiev : Naukova dumka, 1973, in Russian.
[8] Fleck, NA., Smith, RA.: Powder Met.Int., vol. 24, 1991, p. 126.
[9] Staufferand, D., Aharony: Introduction to Percolation Theory. 2nd ed. London : Tailor

& Francis, 1992.
[10] Krasovsky, AY.: Powder Met., 1964, no. 4, p. 167, in Russian.
[11] Šlesár, M. In: Conf. Proc. Deformation and Fracture in Structural PM Materials, vol. 1. Ed. L.Parilák. High Tatras, 1996, p. 85.
[12] Troshenko, VT., Rudenko, VN.: Cermet materials strength and methods of its determination. Kiev : Tekhnika, 1965, in Russian.
[13] Firstov, SA., et. al.: Structure and Strength of Powder Materials. Eds. S.A.Firstov, M. Šlesár. Kiev : Naukova Dumka, 1993, in Russian.
[14] Firstov, SA. In: Conf. Proc. Deformation and Fracture in Structural PM Materials, vol. 1. Ed. L.Parilak. 1996, p. 47.
[15] Podrezov, YN., Lugovoy, NI., Slyunyaev, VN., Verbilo, DG., Chernyshev, LI.: Powder Metallurgy and Metal Ceramics, vol. 39, 2000, no. 3-4, p. 171.
[16] Podrezov, Y., Borodyanska, H., Verbilo, D. In: Proc. Powder Metallurgy World Congress, vol. 5. Granada, 1998, p. 212.
[17] Podrezov, YN., Borodians'ka, HY., Vasylkiv, OO., Firstov, SA. In: Proc. of 2000 PM World Congress. Kyoto, 2000, p. 1159.
[18] Podrezov, YN., Malyshenko, AA., Firstov, SA.: Teor.and Appl.Fract.Mech., vol. 21, 1994, p. 101.
[19] Hahn, GT., Rosenfield, AR.: Trans.AIME, vol. 239, 1967, p. 668.
[20] Podrezov, YN. In: Proc. of Int. Conf. Deformation and Fracture in Structural PM Materials. High Tatras, Slovakia, 1996, p. 147.
[21] Vasilev, AD., Firstov, SA. In: Adv. Multilayered and Fibre-Reinforced Composites, vol. 43. Ed. Y.M.Haddad. Kluwer, NATO, 1998, p. 371.
[22] Vasilev, AD., Firstov, SA., Sotnik, AA. In: Electron microscopy and strength of the materials. Kiev, 1996, p. 11, in Russian.
[23] Podrezov, YN., Lugovoy, NI., Slyunyaev, VN., Minakov, NV.: Theoretical and Applied Fracture Mechanics, vol. 26, 1997, p. 35.
[24] Podrezov, YN., Verbilo, DG., Szafran, M., et al. In: Electron microscopy and strength of the materials. Kiev, 2001, p. 11, in Russian.
[25] Podrezov, YN., Borodians'ka, HY., Vasylkiv, OO., Slyunyaev, VN. In: Proc. of 2000 PM World Congress. Kyoto, 2000, p. 1127.
[26] Podrezov, Y., Verbylo, D. In: Proc. Int. Conf. on Comp. Engineer. Orlando, 1999, p. 579.
[27] Thornton, PH., Magee, CL.: Met.Trans., vol. 6A, 1975, p. 1253.
[28] Maiti, SK., Gibson, LJ., Ashby, MF.: Acta Met., vol. 32, 1984, p. 1963.
[29] Podrezov, YN., Lugovoy, NI., Slyunyaev, VN., Verbilo, DG., Firstov, SA.: Powder Metallurgy and Metal Ceramics, vol. 39, 2000, no. 7-8, p. 407.
[30] Podrezov, YN., Shtyka, LG.: Powder Metallurgy and Metal Ceramics, vol. 39, 2000, no. 1-2, p. 106.
[31] Weber, M., Baumeister, J., Banhart, J., Kunze, HD. In: Conf. Proceedings on Powder Metallurgy PM 94, vol. 3. Paris, 1994, p. 585.
[32] Graninger, R., Simančík, F., Degischer, H. In: Welding Technology, Materials and Materials Testing. Fracture Mechanics and Quality Management, vol. 2. Vienna : University of Technology, 1997, p. 701.
[33] Podrezov, YN., Lugovoy, NI., Slyunyaev, VN., Verbilo, DG., Firstov,SA.: Powder Metallurgy and Metal Ceramics, vol. 39, 2000, no. 8-9, p. 504.